Journal of Engg. Research Vol. 11 No(2B) pp.158-172 DOI:10.36909/jer.14871

Designing of High Voltage Cable Bonding with Intelligence Algorithms to Avoid Cable Insulation Faults and Electroshock in High Voltage Lines

Bahadır AKBAL

Electric and Electronic Engineering Department, Faculty of Engineering and Natural Science, Konya Technical University, Konya , Turkey.

Corresponding Author: bakbal@ktun.edu.tr

Submitted : 17-07-2021

Revised : 03-12-2021

Accepted : 16-12-2021

ABSTRACT

Insulation faults are major problems in high-voltage cable lines. The major factors in insulation faults are the harmonic currents and the metal sheath voltage (MV) that occur on the metal sheath of cables. MV and harmonic distortion should be minimized to prevent insulation faults. Thus, sectional solid bonding with different grounding resistance (SSBr) methods has been developed as a new bonding method for minimizing harmonic current and MV. In addition, SSBr should be optimized by optimizing the minimum MV and harmonic distortion rate of high-voltage cables. Inertia-weighted particle swarm optimization (iPSO), particle swarm optimization (PSO), genetic algorithm (GA), and differential evolution algorithm (DEA) are used for the optimization of SSBr, and three groups of prediction methods are used separately as objective functions of the optimization methods to determine the minimum MV and harmonic distortion; these groups include neural networks, hybrid neural networks, and regression methods. Hybrid neural network with inertia-weighted particle swarm optimization (H-iPSO), linear regression, and feedforward backpropagation neural networks were selected from their groups according to training errors. Solid bonding method, which is widely used for bonding high-voltage cables, is simulated in this study. When solid bonding is used, the maximum harmonic distortion rate is measured as 8.15 %, and the maximum MV is measured as 1086 V. When H-iPSO is used as the prediction method and PSO is used as the optimization method, the maximum harmonic distortion rate is measured as 5.28 %, and the maximum MV is measured as 57 V. Both insulation fault and electroshock can be prevented by the optimized SSBr method.

Keywords: High Voltage Cable Bonding; Hybrid Artificial Neural Network; Optimization.

INTRODUCTION

A high-voltage cable occurs from different layers. The most important layer is the insulation layer. Polyvinyl chloride (PVC), polyethylene (PET), and cross-linked polyethylene (XLPE) insulation materials are used in the insulation layer according to the voltage level. In a high-voltage cable, the insulation layer is covered by the semiconductor layer, which itself is covered by the metal sheath. In high-voltage cable, the insulation faults are generally at the head and end of the line, as verified in consultation with an electricity distribution company. When a line current flows in the conductor of a high-voltage cable, the metal sheath voltage (MV) occurs on the metal sheath, and MV increases towards the end of the line. Thus, the metal sheath is grounded, using cable bonding methods (Ruiz et al. 2007; Jung et al. 2005), to reduce the MV. When the metal sheath of a high-voltage cable is grounded, the metal sheath current (MC) flows on the metal sheath because of the load current. Hence, the cable insulation temperature increases. In addition, if the load current includes the harmonic current (HC), the insulation temperature increases because of the MC and HC (Glover et al. 2012, Mehdi et al. 2014). High-voltage and high-temperature damage the insulation material of the cable (Shuai et al. 2016; Bak et al. 2016). The cable bonding methods indicated in the

literature (IEEE Standard 2014) do not adequately address the insulation faults based on high thermal and electric field effects. Sectional solid bonding method can be used to prevent insulation faults based on high thermal and electric field effects (Akbal 2016; Akbal 2018). However, this method can be used for a maximum of 1-km cable lines (Akbal 2018). Cable grounding is very important for preventing cable insulation faults. Thus, optimal cable bonding should be performed to avoid cable insulation faults. This study proposes a new cable grounding method for the prevention of insulator failures caused by thermal and high electric fields in long cable lines.. Sectional solid bonding with different grounding resistance (SSBr) methods is suggested as a new cable bonding method for long cable lines, and the SSBr method is optimized with intelligent techniques to minimize the high electric field and thermal effects.

In section two, the material and methods used are introduced. The SSBr method developed to prevent cable insulation failures caused by high MV and harmonic currents is described. Artificial intelligence methods used to determine the optimum parameter values in the SSBr method are also introduced, and information regarding the optimization of the SSBr method is provided. Section 3 presents the results and discussion. In this section, the simulation results of the SSBr method optimized using different methods are presented. By evaluating these results, the artificial intelligence methods that provide the best results in the optimization of the SSBr method are determined, and the conclusions are presented in Section 4.

MATERIAL AND METHOD

Several bonding methods for grounding the metal part of a cable have been proposed (IEEE Standard 2014). Single-point bonding is used in short lines, and solid bonding and cross-bonding are used in long lines. However, if the line harmonics are at a high level, MV, HC, and MC increase significantly in the metal parts of the cable owing to the use of these methods. Thus, cable insulation faults and electroshocks are observed in high-voltage cable lines. The SSBr method is suggested for long cable lines that operate under high-harmonic distortion conditions. In the SSBr method, shown in Figure 1, the total cable length is divided into minor parts. The minor part length (L), different grounding resistances (Rg1 and Rg2), and grounding inductances (Lg) are minor parameters. MV is restricted by the optimum minor part length and the current harmonics are restricted by the optimum Lg.

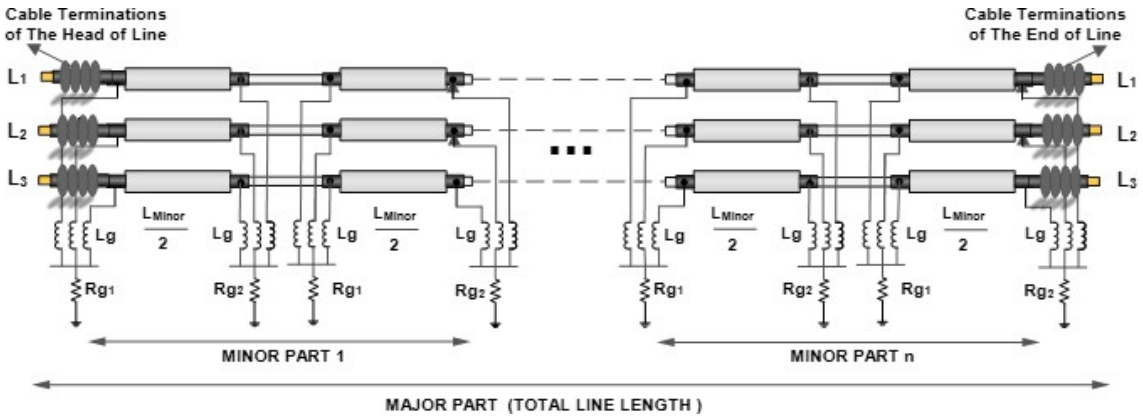

Figure 1. SSBr method.

The high-voltage cable-bonding method should satisfy both economic and technical requirements. Thus, these factors were considered in the design of the optimized SSBr method. If the number of minor parts is minimal, the economic condition is provided. If the MV and harmonic distortion rate are lower than certain limits, technical conditions are provided.

Primarily, L, Rg1, and Rg2 optimization problems should be solved, and the MV should be determined for

L, Rg1, and Rg2 optimizations because these optimizations are performed according to the MV value. The MV value, which can be calculated using the MV formulation, was used as the objective value in the optimization method. However, the affinity of MV formulation is very low (Akbal 2018). Thus, prediction methods were used instead of the formulas. The prediction methods used were neural networks, hybrid neural networks, and regression methods. The predicted MV was used as the fitness value in the optimization process. Neural networks (NN) were used for prediction studies in electrical engineering (Achanta et al. 2012; Weigerta et al. 2010).

Artificial neural networks have learning features, and learning occurs through mathematical modeling. The most basic elements of artificial neural networks are neurons. Neurons work as a transfer function and are modeled using (1).

$$y_i = f_i\left(\sum_{j=1}^{n} w_{ij} \times x_j + b_i\right) \tag{1}$$

The inputs are defined as x_j, weights are defined by w_{ij}, bias is defined as b_i, transfer function is defined as f_i, and output is defined as y_i. Mean square error (MSE), shown in (2), is used to calculate the training errors.

$$E(t) = \frac{1}{n}\sum_{i=1}^{n}(p(i) - o(i))^2 \tag{2}$$

The forecasting error is defined as E(t), the requested value of the output is defined as p(i), and the real value of the output is defined as o(i). The weights that yielded the lowest training error were the most suitable weights for the neural network. Therefore, the weights were updated at each iteration using equation (3). Figure 2 shows how a neuron functions as a transfer function.

$$w_i(t+1) = w_i(t) + \Delta w_i(t) \tag{3}$$

Neural networks consist of an input layer, a hidden layer, and an output layer, as shown in Figure 3. In addition, ANNs have different network structures in artificial neural networks. In this study, feedforward backpropagation (FFBP), layer recurrent (LyR), nonlinear autoregressive network with exogenous inputs (NARX), perceptron (P), and probabilistic (Pb) neural network structures were used.

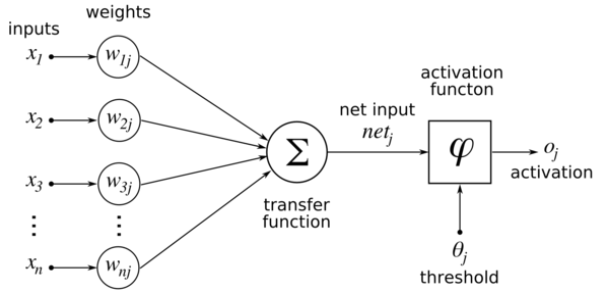

Figure 2. Neuron working

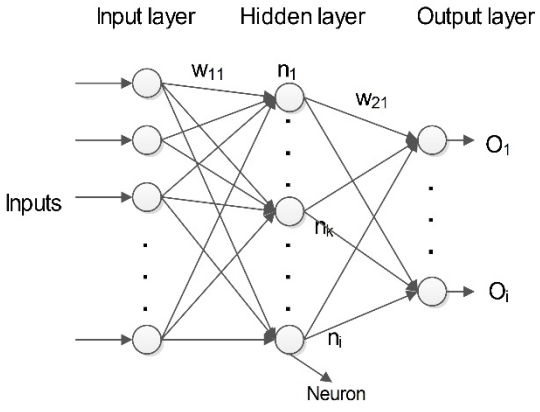

Figure 3. The layers of neural network

In the hybrid artificial neural network method, the weights of the ANN are updated using optimization methods instead of (3). The algorithm for the hybrid ANN method is illustrated in Figure 4.

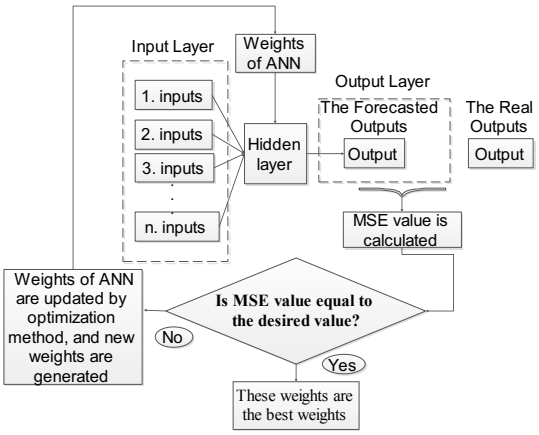

Figure 4. Hybrid ANN algorithm.

The optimization method was used to update the weights of the neural network in the hybrid neural network method to obtain the minimum training error [34,35]. Inertia-weighted particle swarm optimization (iPSO), particle swarm optimization (PSO), genetic algorithm (GA), and differential evolution algorithm (DEA) were used as optimization methods in hybrid neural networks. Neural network and GA hybrid method is called H-GA, the neural network and DEA hybrid method is called H-DEA, the neural network and PSO hybrid method is called H-PSO, and ANN and iPSO hybrid method is called H-iPSO. Regression was another prediction method used in this study, as it has been used to solve prediction problems in electrical engineering (Zhonga et al. 2019; Wang et al. 2012). In regression, the estimation process is based on the relationship between the dependent and independent variables, as shown in equation (4) (Sahinler 2000).

$$Y = a + b.X \tag{4}$$

In Equation (4), the dependent variable is denoted by Y. Therefore, Y is the estimated parameter, and X is the independent variable. In particular, X denotes the estimator variable, where a is the intersection value of the regression line and b is the slope of the regression line. There are different regression structures, and linear regression (LR), robust linear regression (RLR), stepwise linear regression (SWLR), fine tree regression (FTR), linear support vector machine regression (LMVMR), and cubic support vector machine regression (CMVMR) been used as regression methods in prediction studies. The input and output matrices were obtained from the simulation results for the prediction method. The simulation program used was PMCAD/EMTDC to simulate the various cable lines. These matrices were used to train the prediction methods. The minor part length (L), grounding resistances (Rg1 and Rg2), load currents (Ia, Ib, Ic), zero sequence current (ZC), zero-sequence voltage (Ez), total voltage harmonic distortion at the head of line (HV), total voltage harmonic at the end of line (EV), and sheath currents of each phase (Ik1, Ik2,Ik3) are effective for MV (Moutassem et al. 2010; Wei et al. 2018). Thus, the input data are these data, and the output data

re the MV measured in the simulation studies. The matrices are shown in Figure 5.

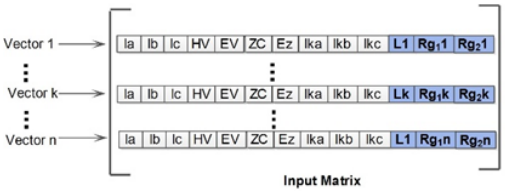

Figure 5. The training process matrices.

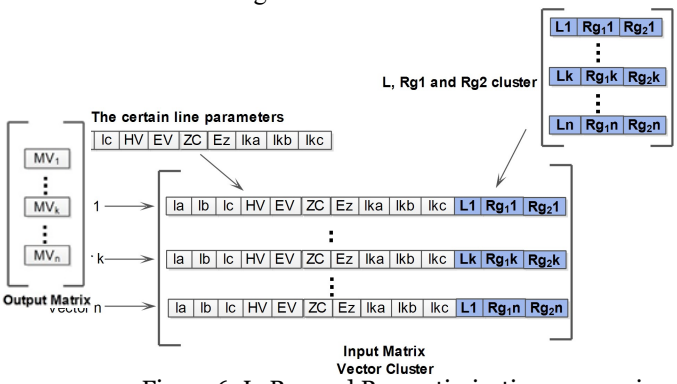

Figure 6. L, Rg1 and Rg2 optimization process input matrix.

The optimum L, Rg1, and Rg2 values were determined using the trained prediction method in the research space. Thus, a new input matrix is essential in the research space. The input matrix is shown in Figure 6. Ia, Ib, Ic, HV, EV, ZC, Ez, Ik1, Ik2, and Ik3 values did not change, and L, Rg1, and Rg2 values were taken from the L, Rg1, and Rg2 matrices. Thus, vector is generated by these parameters. L, Rg1, and Rg2 matrices were generated using the optimization method. In the input matrix, each vector represents a cable line, and the MV of each vector is predicted using the trained prediction method. Therefore, the optimum L, Rg1, and Rg2 values were determined using the trained prediction method based on the MV value of the vector. The output matrix was generated with the forecasted MVs, as shown in Figure 7, and the optimization algorithm shown in Figure 8 was used to optimize L, Rg1, and Rg2. The affinity value in the optimization algorithm shows the vector quality, and is calculated using (5). Where 70.71 V (peak) is the touch voltage limit for a person according to the IEC 479-1 standard.

$$\text{Affinity Value} = 70.71\ \text{V} - \text{the forecasted MV} \tag{5}$$

In Lg optimization, the optimum Lg value is determined according to the minimum current harmonic distortion rate on the metal sheath. If the current harmonic distortion rate is reduced, the cable temperature is reduced, and cable insulation fault is avoided.

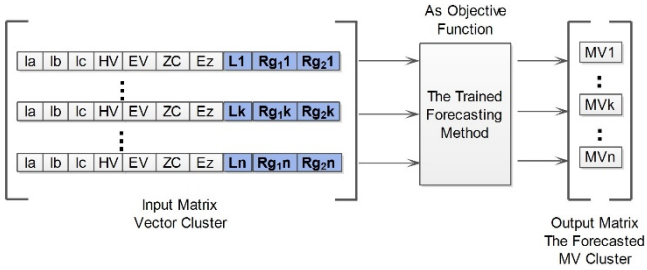

Figure 7. L, Rg1 and Rg2 optimization process output matrix

In addition, the trained prediction method was used as the objective method. Thus, the input and output matrices occur according to different line simulation results. The matrices are shown in Figure 9. The vectors included L, HC, and Lg. The measured current harmonic distortion difference between the cable terminations (Df) was used to generate the output matrix in the training process. The trained prediction method was used to forecast Df, which was used as an objective value in optimization methods. First, a new input matrix is generated to determine the optimum Lg value. Namely, the optimum Lg value is determined by the trained prediction method in the research space. The

new input matrix for the research space is shown in Figure 10. In the vector of the input matrix, L and HC are kept constant because the values of these parameters are certain, and the Lg values of the vectors are changed to find the optimum Lg value. In addition, the Lg matrix was obtained using the optimization method for different Lg values. Df was predicted using the trained prediction method using vectors. The prediction process is illustrated in Figure 11. The best vector was determined according to the minimum Df value of the vector, and the Lg optimization algorithm is shown in Figure 12.

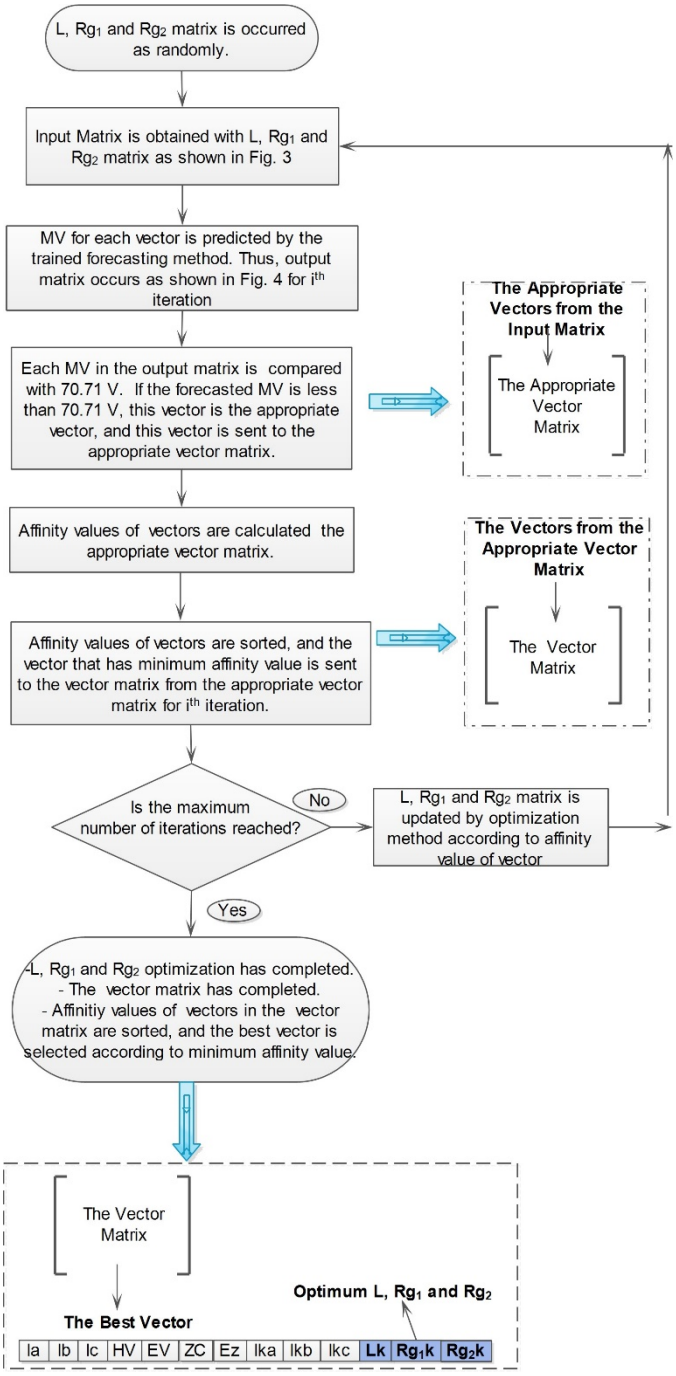

Figure 8. L, Rg1 and Rg2 optimization algorithm

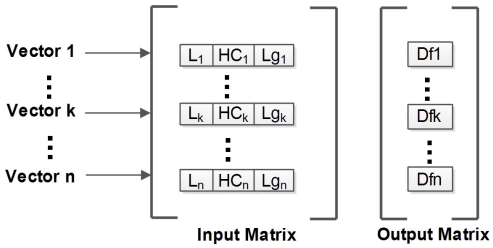

Figure 9. Input and output matrices for training process.

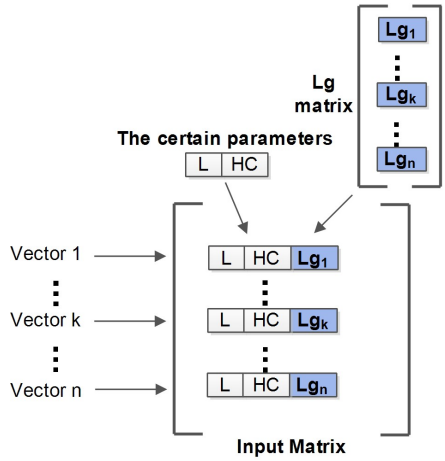

Figure 10. The new input matrix for Lg optimization

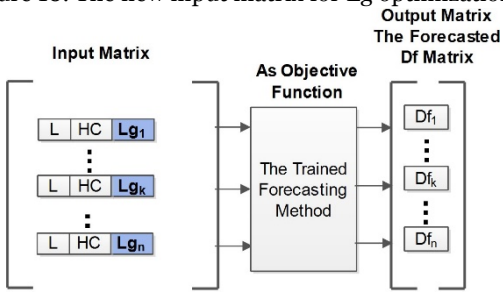

Figure 11. Output matrix for optimization of Lg optimization.

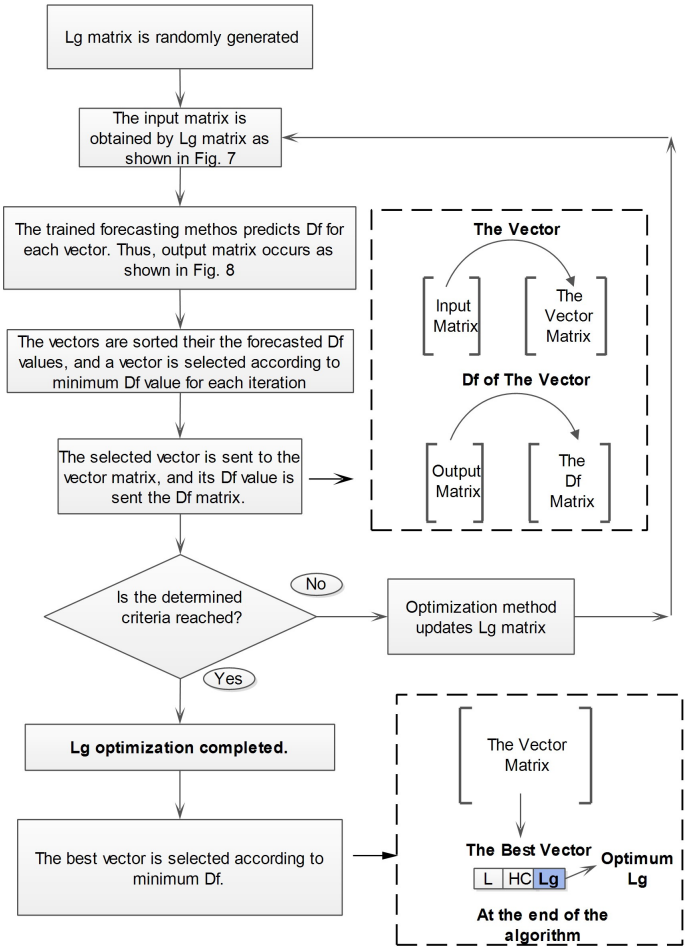

Figure 12. Lg optimization algorithm

RESULTS AND DISCUSSION

In the simulation studies, 61 cable lines were modeled and simulated to obtain the input and output matrices for the training process. The cross-section of the cable used in the cable lines was 1x240mm^2, its insulation material was XLPE, and its operating voltage was 35 kV. After the simulation studies, a 61 × 13 matrix was determined as the input matrix and a 61 × 1 matrix was determined as the output matrix for the training process of L, Rg1, and Rg2 optimization.

The iPSO, PSO, GA, and DEA were used for the optimization of SSBr. The number of iterations for the optimization methods was set to 100 and the number of populations to 50. For PSO and iPSO, the c1 coefficient was set to 2, and the c2 coefficient to 2. In addition, the starting coefficient was 0.4, and the ending coefficient was 0.9, when calculating the inertia weight in the iPSO method. In the GA method, the crossover rate was 0.7, and the mutation rate was 0.01. In the DEA method, the crossover ratio was set to 0.7. The prediction methods were divided into three groups in this study. The first group comprises neural networks, the second group comprises regression methods, and the third group comprises hybrid neural networks. The training errors of the first group of prediction methods are listed in Table 1. It can be observed that the training error of FFBP is lower than that of the other neural network methods. Thus, FFBP was selected as the first prediction method from the first group of prediction methods. The training errors of the second-group prediction methods are listed in Table 2. Notably, the training error of LR is lower than the other regression methods. Thus, LR was selected as the second prediction method from the first group of prediction methods.

Table 1. Training Errors of The First Group

The Prediction Method	Training Errors
FFBP	0.4125
NARX	0.7515
P	5.6140
LyR	5.9893
Pb	5.9893

Table 2. Training Errors of The Second Group.

The Prediction Method	Training Errors
LR	0.3424
RLR	0.4476
FTR	0.8946
LMVMR	1.1522
CMVMR	1.0013

Table3. Training Errors of The Third Group.

The Prediction Method	Training Errors
H-PSO	0.3343
H-DEA	0.5318
H-GA	0.7588
H-iPSO	0.2277

The training error of H-iPSO is lower than those of the other hybrid neural network methods. Hence, H-iPSO was selected as the third prediction method from the third group of prediction methods. The H-iPSO, LR, and FFBP prediction methods are considered separately as the objective functions of the optimization methods in L, Rg1, Rg2, and Lg optimization. The input matrix is a 108 × 3 matrix, and the output matrix is a 108 × 1 matrix for the training process in the Lg optimization. Df is forecasted using trained prediction methods to determine the optimum Lg value. The optimum minor part parameters are listed in Table 4, Table 5, and Table 6. When H-iPSO is considered as the objective function, the optimum minor part parameter values are determined, as listed in Table 4. When LR is considered as the objective function, the optimum minor part parameter values are determined, as listed in Table 5.

Table 4. Optimum L, Rg1, Rg2, and Lg values.

Optimization Method	L (m)	Rg1 (ohm)	Rg2 (ohm)	Lg (H)
iPSO	378	19.9	2.7	0.00091
PSO	364	21.5	2.1	0.00052
GA	249	7.38	9.36	0.03230
DEA	255	20.3	9.13	0.02760

Table 5. Optimum L, Rg1, Rg2, and Lg values.

Optimization Method	L (m)	Rg1 (ohm)	Rg2 (ohm)	Lg (H)
iPSO	246	9.42	15.65	0.0013
PSO	251	8.12	23.54	0.0015
GA	251	13	15	0.0468
DEA	251	6.31	7.74	0.0265

When FFBP is considered as the objective function, the optimum minor part parameter values are determined, as listed in Table 6. After the optimum values are determined, simulations of the optimum minor part parameters are performed to determine the suitability of the determined optimum minor part parameter values. In the simulation studies, the cable line was grounded with SSBr, as shown in Figure 1, and the determined optimum parameter values were used on the bonded cable line. In addition, the total line length of the cable line was 5000 m. MV and HC of the cable terminations were measured in the simulation studies. The common high-voltage line parameters are Ia, Ib, Ic, line voltages (phase-to-ground), total current harmonic distortion in each phase (THDI), and total voltage harmonic distortion in each phase (THDV), as listed in Table 7.

Table 6. Optimum L, Rg1, Rg2 and Lg values.

Optimization Method	L (m)	Rg1 (ohm)	Rg2 (ohm)	Lg (H)
iPSO	250	14.29	21.55	0.0092
PSO	239	10.57	20.51	0.0089
GA	249	21	13	0.0427
DEA	250	22.41	15.07	0.0278

Table 7. Certain Line Parameters.

Line Current (A)	Line Voltage (kV)	THDI (%)	THDV (%)
609	23.4	3.25	3.93
608	23.4	4.93	4.40
598	22.7	2.85	4.66

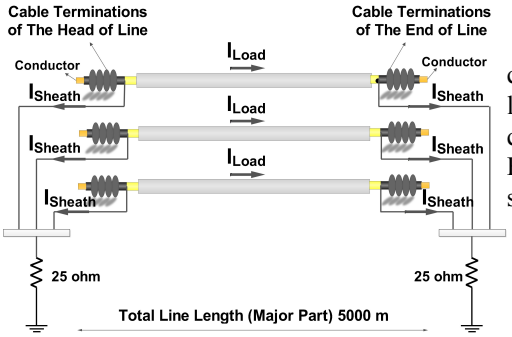

The sheath voltage of solid bonding is lower than that of cross-bonding [15,16,17]. Thus, the bonding of a high-voltage cable line with a length of 5 km was achieved by using solid bonding to compare the optimized SSBr method. The solid bonding shown in Figure 10 is used for the same high-voltage line, and the result of the solid bonding is shown in Table 8.

Table 8. The Result of Solid Bonding

Parameters	HL			EL		
	L1	L2	L3	L1	L2	L3
MV (V)	1086	1081	1023	947	1068	1078
THDI (%)	4.96	8.04	5.23	4.87	8.15	5.48

Figure 10. Solid bonding.

As shown in Table 8, MV and HC increase significantly, so cable faults and electroshocks are observed at the cable termination points, where HL and EL represent the head and end of the line, respectively. In the SSBr optimization, H-iPSO, LR, and FFBP were considered as objective functions, and the determined optimum values, as shown in Tables 4, 5, and 6, respectively, were used in the SSBr method simulations. The simulation results of these optimization methods for H-iPSO as the objective function are presented in Tables 9, 10, 11, and 12. The head-of-the-line cable termination values and the end of the line cable termination values are shown for each phase because voltage increases are generally observed at the cable termination points.

Table 9. Result of iPSO optimization Method

Parameters	HL			EL		
	L1	L2	L3	L1	L2	L3
MV (V)	68	74	63	70	68	69
THDI (%)	4.42	5.72	2.86	4.42	5.73	2.87

Table 10. Result of PSO optimization Method

Parameters	HL			EL		
	L1	L2	L3	L1	L2	L3
MV (V)	52	57	50	52	52	52
THDI (%)	4.97	5.26	2.53	4.98	5.28	2.54

Table 11. Result of GA optimization Method

Table 12. Result of DEA optimization Method

Parameters	HL			EL		
	L1	L2	L3	L1	L2	L3
MV (V)	101	102	93	105	101	104
THDI (%)	2.35	2.97	4.56	2.37	3.04	4.60

Parameters	HL			EL		
	L1	L2	L3	L1	L2	L3
MV (V)	107	104	95	107	103	105
THDI (%)	2.38	3.00	2.86	2.40	3.06	4.67

When H-iPSO was used as the objective function of PSO, the measured MV values on the metal sheath were lower than the touch voltage limit and other optimization methods. In addition, the THDI values did not increase significantly on the metal sheath during PSO optimization. Therefore, cable insulation faults and electroshocks were prevented by the H-iPSO and PSO. The simulation results of the optimization method for LR as the objective function are listed in Tables 13, 14, 15, and 16.

Table 13. Result of iPSO optimization Method

Parameters	HL			EL		
	L1	L2	L3	L1	L2	L3
MV (V)	99	102	91	88	97	100
THDI (%)	5.23	2.71	6.44	5.24	2.73	6.45

Table 14. Result of PSO optimization Method

Parameters	HL			EL		
	L1	L2	L3	L1	L2	L3
MV (V)	96	99	88	86	94	96
THDI (%)	5.16	2.71	6.37	5.17	2.73	6.39

Table 15. Result of GA optimization Method

Parameters	HL			EL		
	L1	L2	L3	L1	L2	L3
MV (V)	100	101	93	91	101	105
THDI (%)	5.34	2.30	5.79	5.35	2.39	5.86

Table 16. Result of DEA optimization Method

Parameters	HL			EL		
	L1	L2	L3	L1	L2	L3
MV (V)	101	102	93	90	101	104
THDI (%)	5.40	2.35	5.95	5.42	2.41	5.99

When LR is considered an objective function of the optimization methods, the MV values on the metal sheath are generally larger than the touch voltage limit. The simulation results of the optimization method when FFBP is considered as the objective function are listed in Tables 17, 18, 19, and 20.

Table 17. Result of iPSO optimization Method

Parameters	HL			EL		
	L1	L2	L3	L1	L2	L3
MV (V)	67	74	58	67	68	65
THDI (%)	3.24	6.17	7.08	3.24	6.17	7.09

Table 18. Result of PSO optimization Method

Parameters	HL			EL		
	L1	L2	L3	L1	L2	L3
MV (V)	72	78	62	72	78	69
THDI (%)	3.36	5.87	7.19	3.36	5.87	7.20

Table 19. Result of GA optimization Method

Parameters	HL			EL		
	L1	L2	L3	L1	L2	L3
MV (V)	99	99	87	90	100	99
THDI (%)	5.33	2.28	5.83	5.36	2.38	5.92

Table 20. Result of DEA optimization Method

Parameters	HL			EL		
	L1	L2	L3	L1	L2	L3
MV (V)	99	101	87	88	99	97
THDI (%)	5.32	2.36	5.98	5.33	2.42	6.03

When FFBP is considered as an objective function of the optimization methods, the MV values on the metal sheath are generally larger than the touch voltage limit. Therefore, cable insulation faults or electroshocks can be observed in the cable line when FFBP or LR is considered as an objective function.

CONCLUSION

Metal sheath grounding prevents cable insulation faults, and the most important factors for insulation faults are MV and HC. Cable insulation fault was prevented by minimizing the MV and current harmonic distortion. Solid bonding was used as a bonding method for grounding a metal sheath, and when solid bonding methods were used for bonding a 5 km cable line, the minimum MV was measured as 947 V, and the maximum MV was 1086 V on the metal sheath. These values are very high for cable lines. In addition, the current harmonic distortion is very high. Namely, the bonding methods used in the literature are inadequate for the minimization of MV and current harmonics, so these methods do not prevent cable insulation faults caused by MV and HC. Thus, an optimized SSBr method was suggested for the minimization of MV and HC. Swarm intelligence and evolutionary optimizations were compared to minimize MV and HC. iPSO and PSO were used for swarm intelligence, and GA and DEA were used for evolutionary

intelligence. When H-iPSO is considered the objective function of PSO for the optimization of SSBr, the maximum MV is 57 V (peak). This value is lower than the touch voltage limit and MVs of the other optimization methods and the solid bonding method. In addition, the current harmonic distortion did not increase significantly at the cable terminations. Hence, cable faults and electroshocks are prevented by the optimized SSBr method used with swarm intelligence.

REFERENCES

Ruiz, J. R., Garcia, A., Morera, X. 2007. A.Circulating sheath currents in flat formation underground power lines. International Conf. Renewable Energies and Power Quality : 1 – 5.

Zhonglei, L., Du, X., Wang, L.,et al. 2012. The calculation of circulating current for the single-core cables in smart grid. IEEE Innovative Smart Grid Technologies – Asia, China : 1 – 4.

Czapp, S., Dobrzynski, K.,Klucznik, J., et al. 2014. Calculation of induced sheath voltages in power cables – single circuit system versus double circuit system. Journal of Information, Control and Management Systems 12: 113 – 123.

Jung, C. K., Lee, J. B., Kang, W. 2007. Sheath circulating current analysis of a cross-bonded power cable systems.J Electr Eng & Technol 2:320 – 328.

Gouramanis, K. V., Kaloudas, C. G.,Papadopoulos, T. A., et al. 2011. Sheath voltage calculations in long medium voltage power cables. IEEE Trondheim Power Tech : 1 – 7.

Jung, C. K., Lee, J. B., Kang, J. W., et al. 2005. Sheath current characteristic and its reduction on underground power cable systems. IEEE Power Engineering Society General Meeting: 2562 – 2569.

Shuai, Z., Houlei, G., Yingtao, Z. 2016. A New Fault-Location Algorithm for Extra-High-Voltage Mixed Lines Based on Phase Characteristics of the Hyperbolic Tangent Function. IEEE Transactions on Power Delivery 31(3):1203-1212.

Jittiphong, K., Atthapol, N. 2017. Fault Groupification on the Hybrid Transmission Line System between Overhead Line and Underground Cable. In: 17th World Congress of International Fuzzy Systems Association and 9th International Conference on Soft Computing and Intelligent Systems (IFSA-MCIS): 1-6.

Jiali, D., Xin, W., Yihui, Z., Lixue, L. 2019. A Novel Fault Location Algorithm for Mixed Overhead-Cable Transmission System Using Unsynchronized Current Data. IEEJ Transactions on Electrical and Electronic Engineering 14:1295-1303.

Yunus, B.2016. Trend adjusted lifetime monitoring of underground power cable. Electric Power Systems Research 143:189-196.

Bessissa, L., Boukezzi, L., Mahi, D. 2016. Influence of Fuzzy Parameters on the Modeling Quality of XLPE Insulation Properties under Thermal Aging. Fuzzy Information and Engineering 8 (1): 101-112.

Bak, C. L., Silva, F. F. 2016. High voltage AC underground cable systems for power transmission – A review of the Danish experience, part 1" , Electric Power Systems Research 140: 984-994.

Bak, C. L., Silva, F. F. 2016. High voltage AC underground cable systems for power transmission

– A review of the Danish experience, part 2" , Electric Power Systems Research 140: 995-1004.

Glover, J. D., Sarma, M. S., & Overbye, T. J. 2012. Power System Analysis and Design. Cengage Leraning, 5th edn.: 428 – 431.

Wei, F., Xiao, K., Qiwei, K. et al.2018. Impact of Neutral Current on Concentric Cable Overloading. IEEE/PES Transmission and Distribution Conference and Exposition (T&D) : 1-5

Zhangping, S., Xing, Z., Fusheng, W., et al. 2015.Modeling and Elimination of Zero-Sequence Circulating Currents in Parallel Three-Level T-Type Grid-Connected Inverters. IEEE Transactions on Power Electronics 30 (2):1050-1063.

Jiangchao, Q.,& Maryam, S. 2015. A Zero-Sequence Voltage Injection-Based Control Strategy for a Parallel Hybrid Modular Multilevel HVDC Converter System. IEEE Transactions on Power Delivery 30(2): 728 – 736.

Mehdi, N., & Gerry, M. 2014. Three-Phase Multi module VSIs Using SHE-PWM to Reduce Zero-Sequence Circulating Current. IEEE Transactions on Industrial Electronics 61(4):1659 – 1668.

IEEE Guide for Bonding Shields and Sheaths of Single-Conductor Power Cables Rated 5 kV through 500 kV, IEEE Standard 2014: 575-2014.

Akbal, B. 2016. Sectional Solid Bonding for Grounding of High Voltage Underground Cables to Reduce the Sheath Current Effects. International Journal of Innovative Research in Engineering & Management 3(2): 103-107.

Akbal, B. 2018. Applications of artificial intelligence and hybrid neural network methods with new bonding method to avoid electroshock risk and insulation faults in high-voltage underground cable lines. Neural Comput & Applic 24(2):32-36.

Akbal, B. 2018. OSSB and Hybrid Methods to Avoid Cable Faults for Harmonic Containing Networks Elektronika Ir Elektrotechnika 29:97 – 105.

Wei, F., Xiao, K., & Qiwei. Z. 2018. Impact of Neutral Current on Concentric Cable Overloading. IEEE/PES Transmission and Distribution Conference and Exposition (T&D): 1-5.

Achanta, R.2012. Long term electric load prediction using neural networks and support vector machines. International Journal of Computer Science and Technology 3: 266 – 269.

Weigerta, T., Tianb, Q., & Lianb, Q. 2010. State-of-charge prediction of batteries and battery – supercapacitor hybrids using artificial neural networks. Journal of Power Sources 196: 4061 – 4066.

Zhonga, H., Wangb, J., Jiac, H., & Muc, L.S. 2019. Vector field-based support vector regression for building energy consumption prediction. Applied Energy 242: 403 – 414.

Kaytez, F., Taplamacioglu, M. C. , Cam, E., & Hardalac, F. Prediction electricity consumption: A comparison of regression analysis, neural networks and least squares support vector machines. Electrical Power and Energy Systems 67: 431 – 438.

Kavaklioglu, K. 2011. Modeling and prediction of Turkey' s electricity consumption using Support Vector Regression. Applied Energy 2011; 88:368 – 375.

Wang, J., Li, L., Niu, T. 2012. Z. An annual load prediction model based on support vector regression with differential evolution algorithm. Applied Energy 94: 65 – 70.

Sahinler, S.2000. En Küçük Kareler Yöntemi ile Doğrusal Regresyon Modeli Oluturmanın Temel Prensipleri.MKÜ Ziraat Fakültesi Dergisi 5 (1-2): 57–73.

Moutassem, W., & Anders, G. J. 2010. Calculation of the eddy current and hysteresis losses in sheathed cables inside a steelpipe. IEEE Trans. Power Delivery 25: 2054 – 2063.

Akbal, B. 2016. Neural-network-based current prediction on high-voltage underground cables. Electronics World 1959:30 – 34.

Benato, R. 2009. Multiconductor analysis of underground power transmission systems: EHV AC cables. Electric Power Systems Research 79:27 – 38.

Marina, S. A., Abderrahim, K., & Fernando, G. 2019. Detection and localization of defects in cable sheath of cross-bonding configuration by sheath currents. IEEE Transactions on Power Delivery 34(4): 1401-1411.

Wei, F., Xiao, K., & Qiwei, Z. 2018. Impact of Neutral Current on Concentric Cable Overloading. IEEE/PES Transmission and Distribution Conference and Exposition (T&D): 1-5.